Raman Spectroscopy on Solids

Aprem Joy, Naga Teja, and T.Gupta

October 2, 2019

Abstract

Contents

1 Introduction

1.1 Phonons

A phonon is a collective excitation in a periodic arrangement of atoms/ions in solids annd some liquids. For our present purpose, we can think of ions being arranged on a crystalline lattice. These phonons are sometimes designated as quasi-particles, and represent quantized modes of vibrations of crystalline solids.

Atoms and ions in a crystal are bound together by coulomb forces. The crystalline lattice represents the ideal structure which defines the equilibrium position of these ions around which they perform small oscillations.

Figure 1 represents a 1D lattice of similar atoms. This system is analogous to setup of coupled harmonic oscillators.

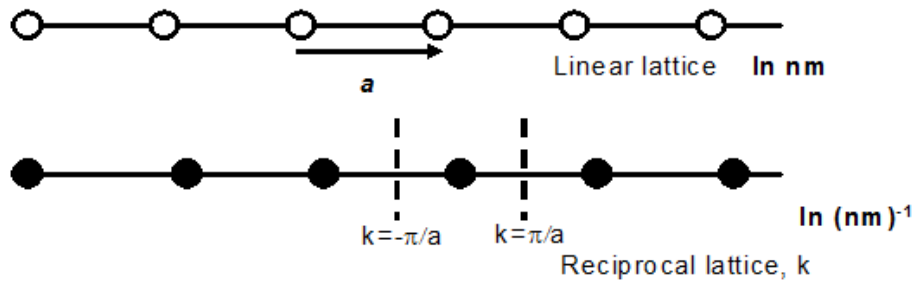

Figure 1: Linear and reciprocal lattice in one dimension. The basic dimension of linear lattice is a, whereas reciprocal lattice is 2 /a. The perpendicular bisector boundaries are $\pm\pi a$ (Brillouin zone boundaries). [1]

The equation of motion for the set of coupled oscillators as shown in Figure 1 is given by:

$$-2Cu_n + C(u_{n-1} + u_{n+1}) = \frac{d^2u_n}{du^2} \tag{1}$$

Here, C is the coupling constant, u_n is the displacement of n^{th} ion from its mean position defined by the Bravais lattice. The Hamiltonian of this system is as defined:

$$H = \sum_i \frac{p_i^2}{2m} + \frac{1}{2}mw^2 + \sum_{ij}(x_i - x_j) \tag{2}$$

The energy associated with the vibrational mode w_k is given by:

$$E_n = \hbar w_k(n + \frac{1}{2}) \tag{3}$$

Here, $\hbar w_k$ is the energy quantum representing a phonon of normal mode k, and n gives the number of such phonons. There can be as many modes as there are degrees of freedom in the system. In the present case of linear chain of n atoms, we have n normal modes. In d dimensional system there will be dn normal modes.

The dispersion relation for such a 1-dimensional chain is given by:

$$w(k) = 2\sqrt{\frac{C}{m}}|sin(\frac{ka}{2})| \tag{4}$$

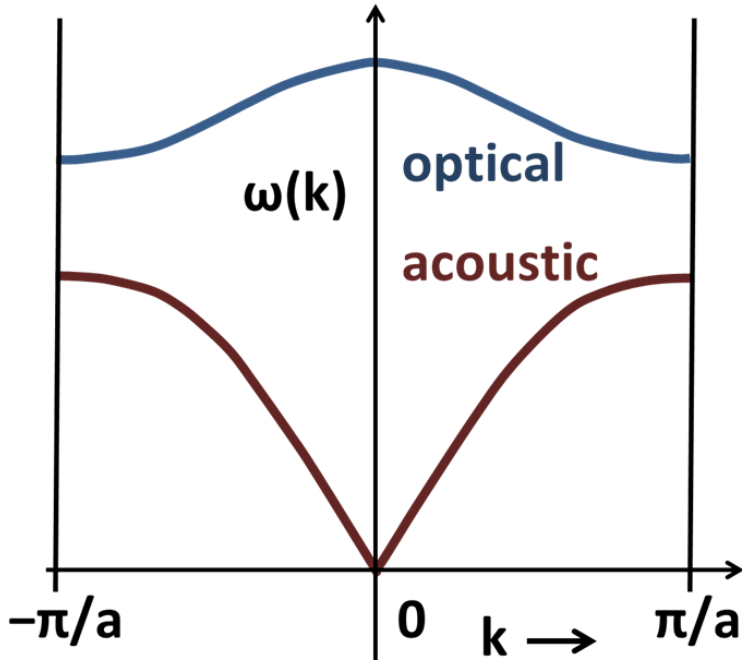

Figure 2: Optical and Acoustic phonon modes for a 1-d chain with diatomic basis

Here, a is the lattice constant. For small k, $w(k) = c_s|k|$, where c_s is the speed of light. That is for small k, the phonon propagates with the speed of light through the lattice. These phonon modes are called acoustic modes. For a 3-d lattice with n atoms, number of acoustic modes is 3 and number of optical modes is 3n-3.

In a 1D-lattice with diatomic basis, the dispersion relation is given by:

$$w(k)^2 = C(\frac{1}{m_1} + \frac{1}{m_2}) \pm C\sqrt{(\frac{1}{m_1} + \frac{1}{m_2})^2 - \frac{4sin^2(ka/2)}{m_1 m_2}} \tag{5}$$

As can be seen in figure 2, the dispersion relationn has two solutions represented by acoustic and optical phonon modes. For Raman spectroscopy, ony the optical modes are relevant. There are 3n-3 optical modes in a 3D lattice with n ions in the basis.

1.2 Raman Spectroscopy

If light of a certainnn frequency w interacts with matter, most of the scattered light has the same frequency w, but there is also a small part that is shifted in frequency [2]. The predominantly elastic scattering interactions are a result of Rayleigh scattering. The much rare Ramann scattering is elastic in nature, and hence shifts the frequency of the scattered photons. If the change is positive i.e. the frequency of the scattered photon increases then it is called as Anti-Stokes scattering, and if the change is negative then the scattering is referred to as Stokes scattering.

The Raman scattering mechanism can be described both classically as well as quantum mechanically. To have the understanding of the finer aspects of the mechanism, we will delve into QM description in the next section.

1.2.1 Classical Interpretation

When an electromagnetic wave encounters a crystal, it gives rise to an oscillation polarization $\vec{P}(t)$ within the crystal given by

$$P = \alpha E \tag{6}$$

Here E is the elctic field of the incidennt wave. This relationship is true for isotropic media. Since ions cannot freely move within the crystalline lattice, the polarizability of a crystal is not isotropic. Hence the strength of the electric field depends on the alignment of the dipole axis with the plane of the incident wave. The polarization then changes to:

$$P_i = \sum_j \alpha_{ij} E_j \tag{7}$$

Note, that plarizability, α_{ij} is a tensor quantity. The polarizability may change according to lattice vibrations, hence each component of α can be expanded into a series with respect to the elongation of the lattice vibration q:

$$\alpha = \alpha_0 + \frac{\partial \alpha}{\partial q}.q + ... \tag{8}$$

Here, α_0 is the contribution that is independent of the amplitude of the phononic vibration. The additional term models the phononic contribution. With an electromagnetic wave given by, $E(t) = E_0(t)cos(w_0 t)$ and phonon of vibrational frequency w_1 leadinng to elongation $q(t) = q_0 cos(w_1 t)$. Substituting this in Polarizability equation, one gets:

$$P = \alpha_0 E_0 cos(w_0 t) + \frac{\partial \alpha}{\partial q}.q_0 cos(w_1 t) E_0 cos(w_0 t) \tag{9}$$

Using trigonometric identities, this can be further expanded to:

$$P = \alpha_0 E_0 cos(w_0 t) + \frac{1}{2} * \frac{\partial \alpha}{\partial q}.q_0 E_0 (cos((w_0 - w_1)t) + cos((w_0 + w_1)t)) \tag{10}$$

This equation contains both Rayleigh and Raman scattering phonons. The Rayleigh scattered phonon is the one with frequency w_0. The other two terms have frequencies shifted upwards $w_0 + w_1$ (Anti-Stokes) and the frequencies shifted downwards $w_0 - w_1$. The classical picture predicts equal intensity for the Stokes and Anti-Stokes processes. In reality, the ratio is temperature dependent as given by $\frac{I_{Anti-stokes}}{I_{Stokes}} \propto e^{-c/T}$. This can be understood by considering quantum mechanical description.

1.2.2 Quantum mechanical interpretation

Now that we have derived the Raman effect using the classical wave interpretation, we can use the quantum particle interpretation to better visualize the process and determine additional information. The Raman effect is described

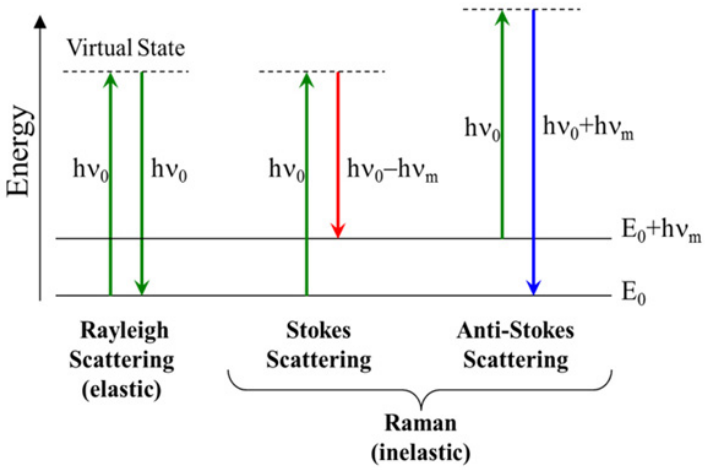

Figure 3: Diagram Representing Quantum Energy Transitions for Rayleigh and Raman Scattering [3]

as inelastic scattering of a photon off of a solid. From the figure 3, we can see that this results from the incident photon exciting the solid into a virtual energy state.

When this occurs, there are three different potential outcomes. First, the lattice can relax back down to the ground state and emit a photon of equal energy to that of the incident photon; this is an elastic process and is again referred to as Rayleigh scattering. Second, the molecule can relax to a real phonon state and emit a photon with less energy than the incident photon; this is called Stokes shifted Raman scattering. The third potential outcome is that the molecule is already in an excited phonon state, is excited to a higher virtual state, and then relaxes back down to the ground state emitting a photon with more energy than the incident photon; this is called Anti-Stokes Raman scattering. Due to the fact that most molecules will be found in the ground state at room temperature, there is a much lower probability that a photon will be Anti-Stokes scattered. As a result, most Raman measurements are performed considering only the Stokes shifted light.

The probability of finding n phonons of frequency w follows a Boltzmann distribution with $P(n) \propto e^{\frac{-E_n}{k_b T}}$, the relative intensities of Stokes and Anti-stokes processes are also related by probabilities of finding solid in excited and ground states respectively. Hence,

$$\frac{I_{Anti-stokes}}{I_{Stokes}} \propto e^{-E/k_b T} \tag{11}$$

From the equation, one can see that Anti-Stokes scattering does not take place when Temperature tends to 0K.

1.3 Raman Tensor

Thr Raman tensor is characteristic to the symmetry group of the crystal. THe symmetry is described relative orientation of hte crystallographic axes (a,b and

c) and the direction of the ingoing and the outgoing beam abd their polarization axes (x,y and z). Raman tensor matrix written in Porto notation as follows

$$M = \begin{bmatrix} aa & ab & ac \\ ba & bb & bc \\ ca & cb & cc \end{bmatrix} \tag{12}$$

1.3.1 Si (100)

The Raman tensor for Si(100) is:

$$R_{100} = \begin{bmatrix} 0 & f & 0 \\ f & 0 & 0 \\ 0 & 0 & 0 \end{bmatrix} \tag{13}$$

Assume $\hat{e_i}$ and $\hat{e_s}$ be the unit vectors of the polarization of the incident and scattered light, respectively. Then, the Raman scattering intensity is proportional to

$$I \propto |\hat{e_i} R \hat{e_s}|^2 \tag{14}$$

If $\hat{e_i} = (sin(\theta_i), cos(\theta_i), 0)$ and $\hat{e_s} = (sin(\theta_s), cos(\theta_s), 0)$, then

$$I \propto f^2 sin^2(2(\theta_i - \theta_s)) \tag{15}$$

1.3.2 Si (111)

Si (111) belongs to a different symmetry group than Si (100). Hence, the Raman tensor is different owing to different vibrational modes being excited. We can find the Raman tensor for Si (111) by rotating the Raman tensor for Si (100) along the (0,0,1) direction into (1,1,1) direction. The rotation matrix is given by

$$O = \begin{bmatrix} \frac{1}{6}(\sqrt{3}+3) & \frac{1}{6}(\sqrt{3}-3) & \frac{1}{\sqrt{3}} \\ \frac{1}{6}(\sqrt{3}-3) & \frac{1}{6}(\sqrt{3}+3) & \frac{1}{\sqrt{3}} \\ -\frac{1}{\sqrt{3}} & -\frac{1}{\sqrt{3}} & \frac{1}{\sqrt{3}} \end{bmatrix} \tag{16}$$

Rotating R_{100} by M matrix,

$$R_{111} = M^{-1} R_{100} M = f. \begin{bmatrix} -1 & 0 & 0 \\ 0 & -1 & 0 \\ 0 & 0 & 2 \end{bmatrix} \tag{17}$$

which gives the Raman intensity using eq 14 to be

$$I_{111} \propto f^2 \tag{18}$$

2 Experiment

2.1 Setup

We use a laser of wavelength 532 nm as the source. Polarizer and analyzer are used for the incident and the scattered light respectively to change the polarization directions with respect to the sample crystal axes. We use attenuators

to reduce the high incoming beam intensity so as to not damage the detector which is a CCD photodetector. The incoming falls on the sample after being reflected on a mirror and the scattered light passes through columnating and focusing lens system to fall on the entrance slit whose width can be controlled. We also use an edge filter to cut off the Anti-Stokes-scattered light. The light comes out from the slit and is detected by the CCD detector.

3 Analysis

3.1 Measurement and Calibration

While performing the experiment, we took measurements of two samples of silicon with 100 and 111 geometry. The polarization angles of the polarizer and the analyzer were adjusted so that we get maximum intensity output. We use the measurements to first calibrate the setup and check for offsets in the peak wave number. The setup was calibrated in such a manner that the line should have been detected at $521cm^-1$, but because of imperfect alignment we obtained the peak at around $530cm^-1$ for Si100 and $529cm^-1$ for Si111 (as shown in figure 6.

3.1.1 Si[100]

We find there is a peak at $531nm$. The height of the peak changes with the angle, which can be seen in the Figure 4.

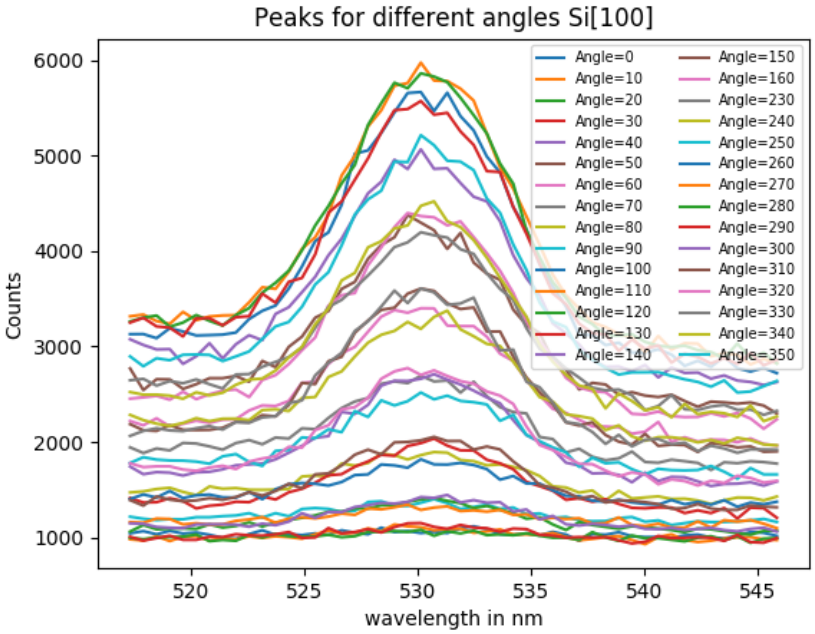

Figure 4: The peaks at various angles for Si[100].

3.1.2 Si[111]

We see similar behavior in this part though the data is heavily dominated by noise for the case of Si[111]. The peak can be observed at $530nm$ in Figure 5.

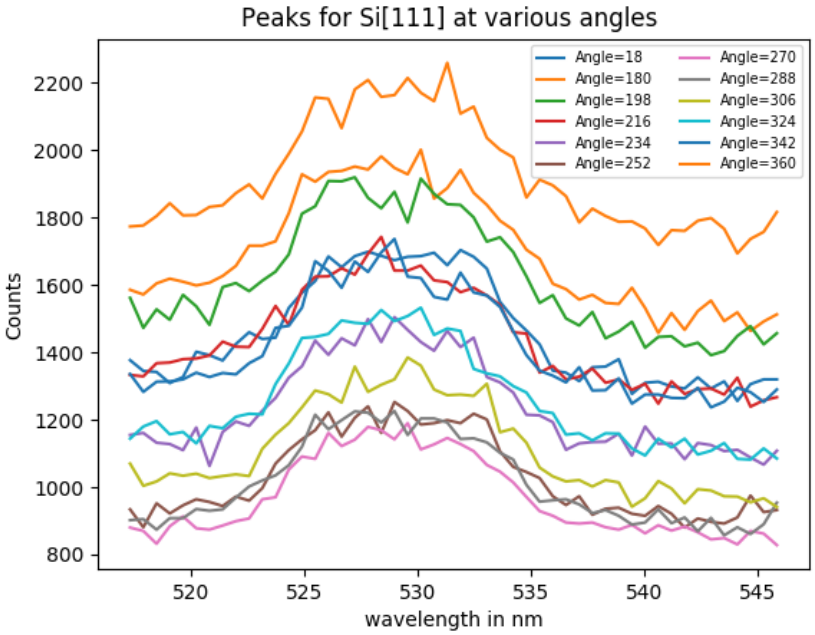

Figure 5: The peaks at various angles for Si[111].

3.2 Resolution of the spectrometer

The observed data was fitted with three different functions to determine the peak position and width of the Raman lines. These functions include, Gaussian, Lorentzian, and Voigt profile which is a weighted combination of Gaussian and Lorentzian functions.

1. **Gaussian:** $f(x) = A_G e^{-\left(\frac{x-\mu_G}{\sigma_G}\right)^2} + C_G$
2. **Lorentzian:** $g(x) = \frac{A_L}{1+(\frac{x-\mu_L}{\sigma_L})^2} + C_L$
3. **Voigt:** $h(x) = af(x) + (1-a)g(x)$

where we take A_L, A_G as the respective amplitudes of Lorentzian and Gaussian, similarly σ, μ correspond to their respective means and variances.

Why we fit the peaks with Voigt Profile? Consider the relaxation time for an excitation to be τ_r and coherence time to be τ_c. The first one is the time taken for the excitation to be effectively dissipated into the system, the second is time it takes for the excitation to start becoming incoherent due to the randomness of the environment. Even though both have the same effect of making the reading on the spectrometer zero, they have different effects on the spectrum.

If we consider the case $\tau_c >> \tau_r$, this happens in solids where the lattice is very regular and hence, excitations can be stable for a long time. In this case

the profile is a Gaussian. In the case where $\tau_r >> \tau_c$, which happens in fluids, we have irregularity in the way atoms are arrange which results in very fast incoherence to arise. In this case, the profile is Lorentzian.

In a real solid, the atoms are neither perfectly ordered nor in the totally disordered like the fluid. Hence, we use a linear superposition of both of them. Also, we can attempt to quantify the "Fluidness" of the solid from the ratio $A_L : A_G$.

We consider the region around the maximal peak which is at 10^O for the next part.

3.2.1 Si[100]

We fit the peak with Gaussian, Lorentzian and Voigt profiles as discussed above. Note the parameters below.

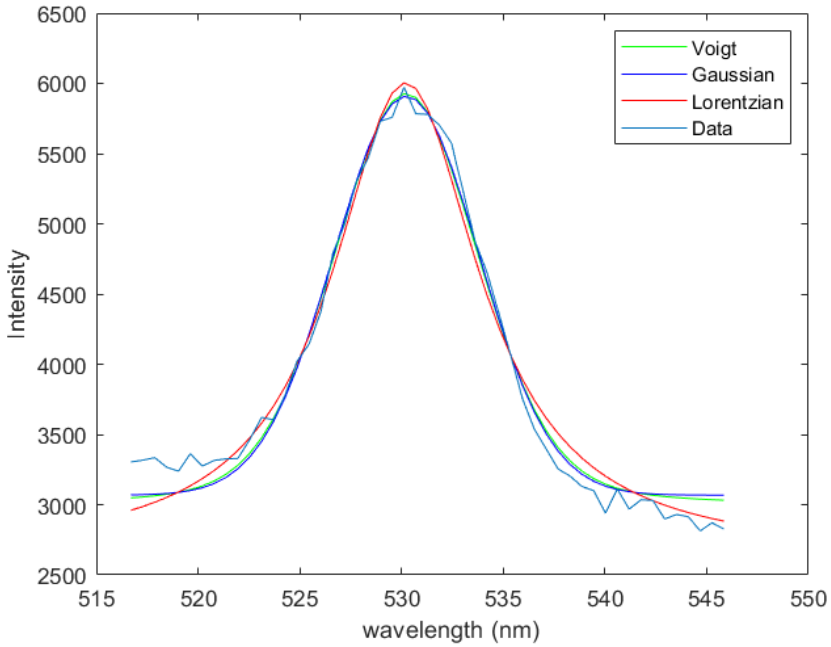

Figure 6: The peak and fitting for Si[100] at 10^o.

A_L	μ_L	σ_L	C_L	A_G	μ_L	σ_G	C_G	a
3373.1	530.2	4.4	2532.5	2840.7	530.2	5.0	3067.8	0.804

Table 1: Parameters of the Lorentian, Gaussian and Voigt fits for Si[100]

3.2.2 Si[111]

We fit the peak with Gaussian, Lorentzian and Voigt profiles as discussed above. Note the parameters below. We would like to note that we find that the fit is

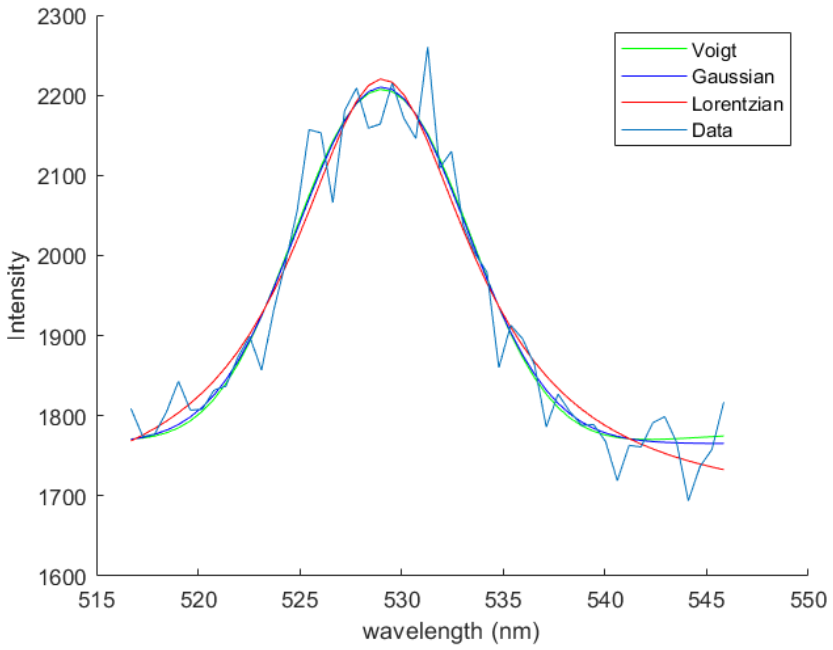

Figure 7: The peak and fitting for Si[111] at 0^o.

A_L	μ_L	σ_L	C_L	A_G	μ_L	σ_G	C_G	a
538.7	529.1	5.4	1681.8	445.1	529	5.9	1765.2	1.0

Table 2: Parameters of the Lorentian, Gaussian and Voigt fits for Si[111]

essentially Gaussian $a = 1$. This, we guess is due to the high noise in our data.

3.2.3 Raman Tensor

As discussed in Section 1.3, we can calculate the Raman Tensor from the intensity v/s angle plot.

3.2.4 Si[100]

Using Eq. 15, we can obtain the value of f by fitting the intensity v/s angle plot with a sinusoidal function and obtain the Raman tensor value 'f'. This is done in fig.9 The value of f calculated from the fit is

$$f = 35.9$$
$$\omega = 2.01$$

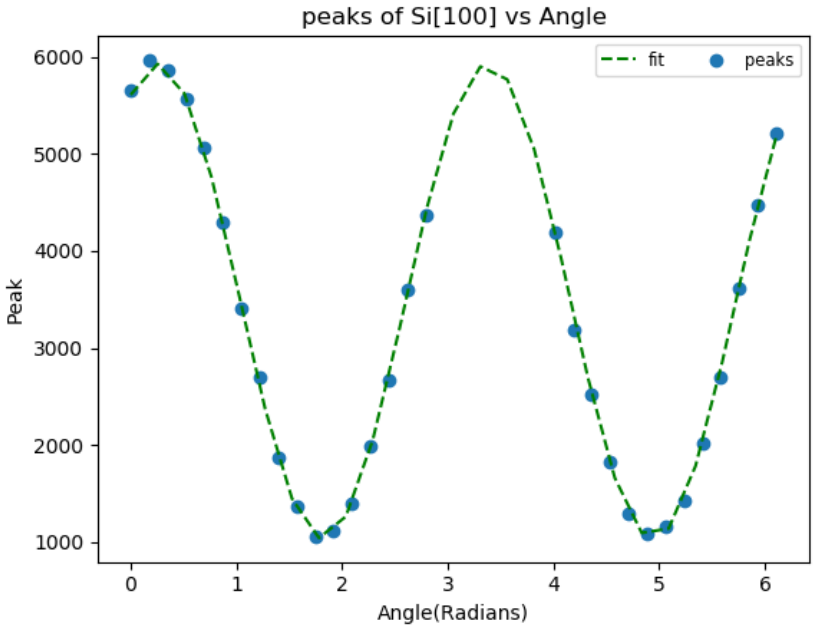

Figure 8: Peaks at different angles of the polarizer for Si[100].

3.2.5 Si[111]

As described in Eq.18, the value of Raman tensor f can be calculated by taking the mean square root of the Intensity values for various angles.

Even though we expect the Intensity to be independent of the analyzer angle for Si[111], the graph 9 shows deviation from this behaviour. But this variation is small when compared with the Si[100] plot as shown in fig.10 and can be approximated to be independent of the angle

Intensity wrt angle: The plots for intensity vs angles are fitted with the below fitting function for full generality

$$f(x) = A(sin(\omega(x + \phi)))^2 + C$$

where ω is "frequency" of variation. The value of f is obtained as

$$f = 39.5$$

For Si[111], we find that the dependence of peaks on the angle is way less pronounced than that of Si[100]. Hence agrees with the theoretical prediction but with some error. The range of variation of the Intensity can be seen in 9. But the comparison of graphs of Si[100] and Si[111] (10) reveals that the I_{111} can be approximated to almost independent of the analyzer angle.

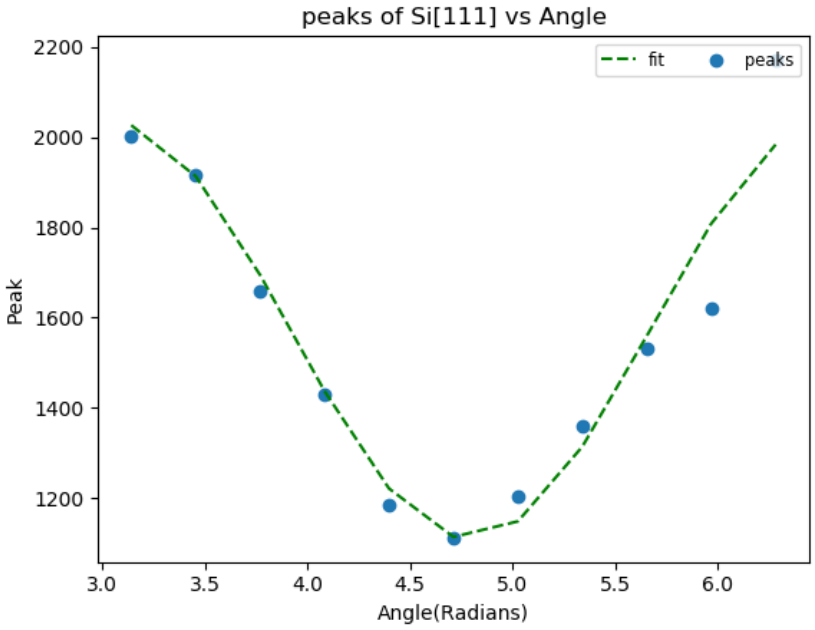

Figure 9: Peaks at different angles of the polarizer for Si[111].

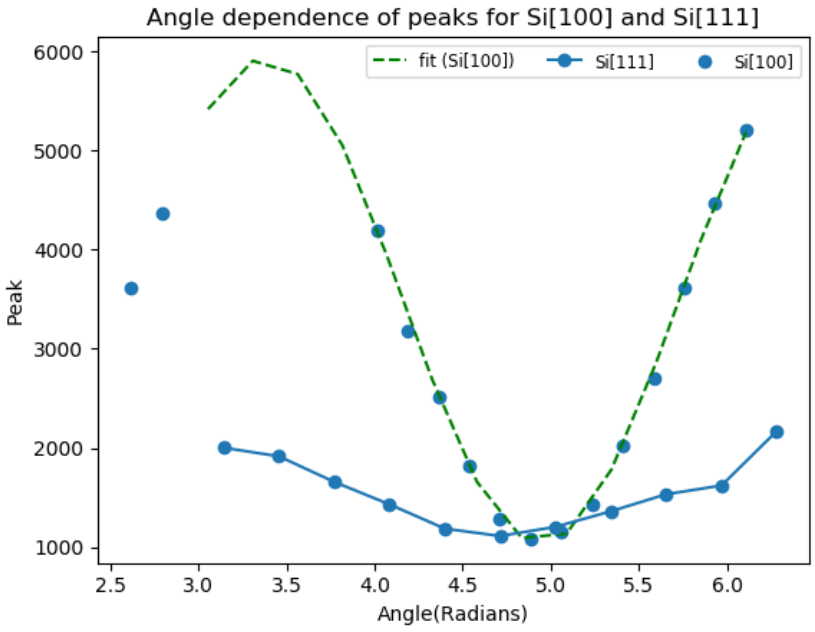

Figure 10: Comparison of peaks vs angles for Si[100] and Si[111].

4 Discussion and Conclusion

In this experiment, we learned about the experimental technique of Raman spectroscopy by measuring the Raman spectra of two different crystal structures of Si which have different symmetries and thus diffErent Raman tensors.
We first calibrated the optical setup by measuring the Raman spectra of the samples and obtained the peaks for various polarizer-analyzer angles. A shift of around $10nm$ was found in the peak wavelength from the true value. We fitted the peaks using Gaussian, Lorentzian and Voigt profiles. The Intensity v/s analyzer angle was plotted and it was observed that the intensity variation is more pronounced in Si[100] than Si[111] and follows a $\sim sin^2(\omega t)$as predicted theoretically. Si[111], however did show some deviation from the theoretical prediction which could be due to noise and imperfect alignment of the optical setup. But this was observed to be insignificant when compared to the angle dependency of intensity in Si[100]. Finally, we used these fits to calculate the Raman tensor value.

References

[1] "https://nptel.ac.in/courses/115102025/2."

[2] P. . Institute, "Solid state advanced praktikum pre-lab manual," 2018.

[3] "http://bwtek.com/raman-theory-of-raman-scattering/."

[4] J. Rossat-Mignod, L. Regnault, M. Jurgens, C. Vettier, P. Burlet, J. Henry, and G. Lapertot, "Neutron scattering study of yba2cu3o6+ x single crystals," *Physica B: Condensed Matter*, vol. 163, no. 1-3, pp. 4–8, 1990.

[5] B. A. Ruzicka, L. K. Werake, H. Samassekou, and H. Zhao, "Ambipolar diffusion of photoexcited carriers in bulk gaas," *Applied Physics Letters*, vol. 97, no. 26, p. 262119, 2010.